^{3}He pO_2 Mapping Is Limited by Delayed-Ventilation and Diffusion in Chronic Obstructive Pulmonary Disease

Helen Marshall,[1] Juan Parra-Robles,[1] Martin H. Deppe,[1] David A. Lipson,[2] Rod Lawson,[3] and Jim M. Wild[1]*

Purpose: Lung pO_2 mapping with ^{3}He MRI assumes that the sources of signal decay with time during a breath-hold are radiofrequency depolarization and oxygen-dependent T_1 relaxation, but the method is sensitive to other sources of spatio-temporal signal change such as diffusion. The purpose of this work was to assess the use of ^{3}He pO_2 mapping in patients with chronic obstructive pulmonary disease.

Methods: Ten patients with moderate to severe chronic obstructive pulmonary disease were scanned with a 3D single breath-hold pO_2 mapping sequence.

Results: Images showed signal increasing over time in some lung regions due to delayed ventilation during breath-hold. Regions of physically unrealistic negative pO_2 values were seen in all patients, and regional mean pO_2 values of -0.3 bar were measured in the two patients most affected by delayed ventilation (where mean time to signal onset was 3–4 s).

Conclusions: Movement of gas within the lungs during breath-hold causes regional changes in signal over time that are not related to oxygen concentration, leading to erroneous pO_2 measurements using the linear oxygen-dependent signal decay model. These spatio-temporal sources of signal change cannot be reliably separated at present, making pO_2 mapping using this methodology unreliable in chronic obstructive pulmonary disease patients with significant bullous emphysema or delayed ventilation. **Magn Reson Med 71:1172–1178, 2014. © 2013 Wiley Periodicals, Inc.**

Key words: hyperpolarized ^{3}He; partial pressure of oxygen; chronic obstructive pulmonary disease; delayed-ventilation; diffusion

The partial pressure of oxygen (pO_2) in the lung airspaces depends on ventilation and perfusion matching and is a regional indicator of gas exchange. Hyperpolarized ^{3}He MRI pO_2 mapping has been shown to provide quantitative, regional measures of pO_2 in healthy volunteers (HVs) (1–4), which are physiologically plausible. The method assumes that all signal depletion during a breath-hold is due to radiofrequency (RF) depolarization and oxygen-dependent T_1 effects (5) and these effects can be separated to calculate the regional pO_2 using typically a linear (1), or exponential (6), oxygen-dependent signal decay model.

The method is, however, also sensitive to other sources of temporal signal change during the breath-hold acquisition time. pO_2 mapping methods by definition require time resolved images to be separated by a delay time Δt, which is of the same order of magnitude as the ^{3}He T_1 in air $\approx$ 20 s (1,5). Hence, inter-frame delays of 2–5 s are typically used to measure the pO_2 with ^{3}He. On this time scale, inter-slice diffusion of gas with different polarization has been shown to be a source of significant error in slice selective 2D pO_2 acquisitions leading to an underestimation of pO_2 values (4). This can be mitigated by using a 3D sequence (4) where the whole lung experiences the same RF history. Nevertheless, inter-pixel diffusion is still a source of error in 3D pO_2 mapping if the pixel size Δz, is such that $\Delta z \approx z_{rms} = \sqrt{2D\Delta t}$, where D is the characteristic diffusion coefficient on the time and microstructural length scale of the experiment. For free ^{3}He diffusion in air $D = 0.86$ cm^2/s (7), whereas smaller apparent diffusion coefficients (ADCs) are characteristic of longer diffusion times in healthy acinar tissue when measured with longitudinal diffusion weighted magnetization pulse sequences (8–11). Similarly, any other change in signal decay, which is not related to oxygen concentration or RF depolarization, such as a delayed in-flow of gas into the region of interest (ROI), could cause errors in the pO_2 values calculated with the technique.

^{3}He pO_2 mapping has been used to image patients with bronchiolitis obliterans (12) and lung transplant (12,13), and several studies have performed pO_2 mapping in patients with chronic obstructive pulmonary disease (COPD) (13–17). COPD is characterized by abnormalities of air-flow and elevation in regional gas ADC related to emphysema in the alveolar spaces (18). Movement of gas within the lungs of COPD patients during breath-hold was recently observed, with initially unventilated defects filling with gas over the period of a single breath hold (19).

The aim of this work was to investigate the effects of delayed-ventilation and diffusion in ^{3}He pO_2 mapping in patients with moderate to severe COPD. It was hypothesized that gas movement and delayed ventilation during static breath-hold in regions of emphysematous and partially obstructed lung would cause errors in the pO_2 values returned by the technique. ^{3}He 3D pO_2 mapping was performed in patients with moderate to severe COPD as defined by the Global initiative for chronic Obstructive Lung Disease guidelines. Paradoxical findings in the

[1]Department of Academic Radiology, University of Sheffield, Sheffield, South Yorkshire, UK.

[2]GlaxoSmithKline, King of Prussia, Pennsylvania, USA.

[3]Department of Respiratory Medicine, Sheffield Teaching Hospitals NHS Trust, South Yorkshire, UK.

Grant sponsor: GlaxoSmithKline; Grant number: RES111175; Grant sponsor: UK EPSRC; Grant number: EP/D070252/1.

*Correspondence to: Jim M. Wild, Ph.D., Department of Academic Radiology, C Floor, Royal Hallamshire Hospital, Glossop Road, Sheffield, South Yorkshire S10 2JF, UK. E-mail: j.m.wild@sheffield.ac.uk

Received 17 August 2012; revised 7 March 2013; accepted 29 March 2013

DOI 10.1002/mrm.24779

Published online 9 May 2013 in Wiley Online Library (wileyonlinelibrary.com).

Table 1
Demographics and FEV1 Values of the Patients (A–J) and Three Healthy Volunteers (HV1–HV3)

Subject	Age (years)	Sex	Height (cm)	Weight (kg)	Smoking history (pack years)	FEV1 (L)	FEV1 % predicted
A	55	F	155	62	30	0.83	39
B	64	F	160	97	50	0.72	34
C	64	M	163	53	25	1.50	56
D	62	M	183	98	35	1.08	30
E	68	M	169	83	90	1.54	55
F	64	M	170	87	20	1.39	47
G	63	F	157	70	50	0.72	35
H	58	M	172	99	35	2.61	81
I	50	F	156	89	40	1.69	74
J	58	F	159	77	20	0.99	45
HV1	26	M	183	80	0	5.28	113
HV2	29	M	187	75	0	5.02	107
HV3	35	M	170	65	0	3.78	96

measured regional pO_2 values were observed confirming the technique is prone to error in diseased lungs where gas ventilation is delayed or inter-voxel gas diffusion is spatially unconstrained by emphysematous disruption to the lung microstructure.

METHODS

Ten patients with COPD were scanned. The inclusion criteria were COPD without other significant respiratory disease as diagnosed by a respiratory physician, postbronchodilator ratio of forced expiratory volume in 1 s (FEV1) to forced vital capacity <0.7, postbronchodilator FEV1 $\geq$30% and $\leq$80% of predicted, cigarette smoking history of $\geq$10 pack-years, and resting pulse oximeter oxygen saturation of $>$90% on room air. Patient demographics and FEV1 values are shown in Table 1.

Imaging was performed on a 1.5 T whole body MRI system (GE HDx, Milwaukee, WI) equipped for hyperpolarized ^{3}He imaging. ^{3}He was polarized on site to around 25% using rubidium spin-exchange apparatus (GE Healthcare, Amersham, UK) under UK regulatory license. Imaging was conducted with national research ethics committee approval. Patients were positioned in a ^{3}He quadrature transmit-receive vest coil (Clinical MR Solutions, Brookfield, WI). A mix of 200 mL hyperpolarized ^{3}He and 800 mL N_2 was inhaled from a state of relaxed expiration, and ^{3}He images were acquired using a single breath-hold sequence based on (4,20). 3D coronal spoiled gradient echo images with full lung coverage were acquired with field of view = 35 cm, flip angle = 1°, 16 × 20 mm slices, in-plane matrix = 64 × 32, planar spatial resolution = 5.5 × 10.9 mm, bandwidth = 62 kHz, echo time = 0.8 ms, and pulse repetition time = 2.5 ms. The 3D imaging volume was acquired at 6 time points during the breath-hold with inter-image delay times of τ_1 = 1.3 s and τ_2 = 4.5 s (Fig. 1). Three HVs were scanned with the same protocol.

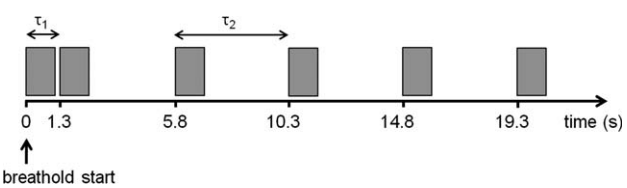

FIG. 1. Sequence timing diagram for pO_2 mapping within a single breath-hold. 3D spoiled gradient echo sequence with inter-image delay times of τ_1 = 1.3 s and τ_2 = 4.5 s. 3D imaging volume represented as a grey rectangle.

Images were masked to segment the lung from background noise according to the signal-to-noise ratio (SNR) of the final dynamic 3D image data (21), and fit pixel-by-pixel in Matlab (MathWorks, Natick, MA) to calculate regional starting pO_2 maps in a coronal plane as described in (4). The time dependence of pO_2 during a breath-hold was assumed to be linear and given by $pO_2(t) = p_0 - Rt$, where p_0 is the initial partial pressure and R is the rate of oxygen extraction by perfusion (1,4). To observe the temporal signal behavior of the imaging data, ROIs were prescribed. The mean ROI signal normalized to the mean ROI signal of the first time point was plotted with respect to time and corresponding mean pO_2 values were calculated.

A rough estimate of the size of error caused by delayed ventilation was made, by using the magnitude of the physically unrealistic negative pO_2 values as a lower limit on the estimate of error. The mean negative pO_2 value was compared with the time to signal onset parameter used in (19) to assess the influence of the temporal aspect of delayed ventilation. The effect of breath-hold time on the measured pO_2 values was assessed by generating pO_2 maps using all 6 time points (21 second acquisition) and comparing them to those made using only the first 4 time points (12 second acquisition).

RESULTS

Figure 2 shows maps of the initial pO_2 (p_0 at time $t = 0$), from a healthy volunteer (HV1) and from a COPD patient (patient A). The pO_2 map from the HV (a) was relatively homogeneous with mean values of 0.13 bar in the left lung and 0.14 bar in the right lung. In the COPD patient, negative pO_2 values were returned from several regions of the lung (d).

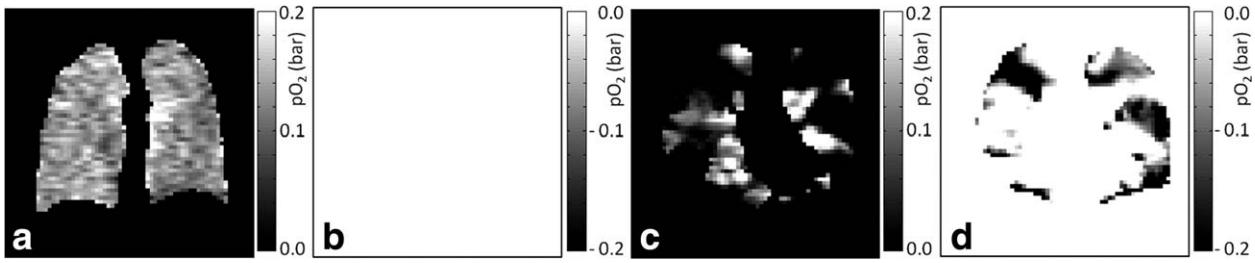

FIG. 2. pO_2 maps from (**a**, **b**) a healthy volunteer, and (**c**, **d**) a COPD patient (Patient A) with gas movement in the lungs during breath-hold. The panels (a) and (c) show positive pO_2 values, and (b) and (d) show negative "pO_2 values" where signal increases over time.

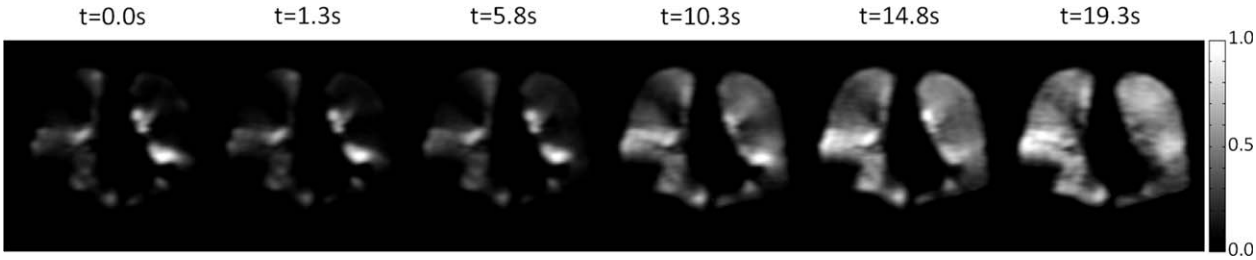

FIG. 3. The ^{3}He signal time-course images of the COPD patient shown in Figure 2. The signal is normalized to the maximum signal value at each time point.

The pO_2 maps from all HVs were relatively homogeneous and predominantly had values similar to those published previously for HVs (1,4). A small region with negative pO_2 was seen near the diaphragm in HV3 due to a slight downward movement of the left lung base during breath-hold. Elevated pO_2 values were observed near the heart in HV2 and HV3, which may be caused by cardiac motion.

The source ^{3}He time-course images from patient A (Fig. 3) show gas moving into initially unventilated defects during the course of the static breath-hold. Initially, the gas distribution is inhomogeneous with regions of ^{3}He hyper-intensity and voids but during the breath-hold it becomes more evenly distributed as regions, which were initially poorly ventilated, become ventilated.

Analysis of the ROI signal time-courses (Fig. 4) showed that signal increased over time in regions which returned negative pO_2 values (d, solid and dotted lines) which is clearly an unrealistic physical situation if $T_1(pO_2)$ and RF pulse depolarization are assumed to be the only sources of signal change during breath-hold. Signal ROI plots demonstrate that even regions away from obvious slow-filling ventilation defects can experience a delay before peak signal is reached (e.g., d, dotted line). pO_2 values from ROIs in (c) were 0.17 (dashed line), 0.10 (dash-dot line), −0.10 (dotted line), and −0.40 bar (solid line). If data were masked according to the SNR of the first dynamic volume, rather than the last, regions of negative pO_2 values would not be included in the calculated pO_2 maps. However, the adjacent lung regions would remain affected by gas movement from them into the initially unventilated defects in a similar manner.

Figure 5 shows the first and last time-point ^{3}He source images and the calculated pO_2 maps for the other nine COPD patients. Gas movement during static breath-hold was observed in some parts of the lung in all of the 10

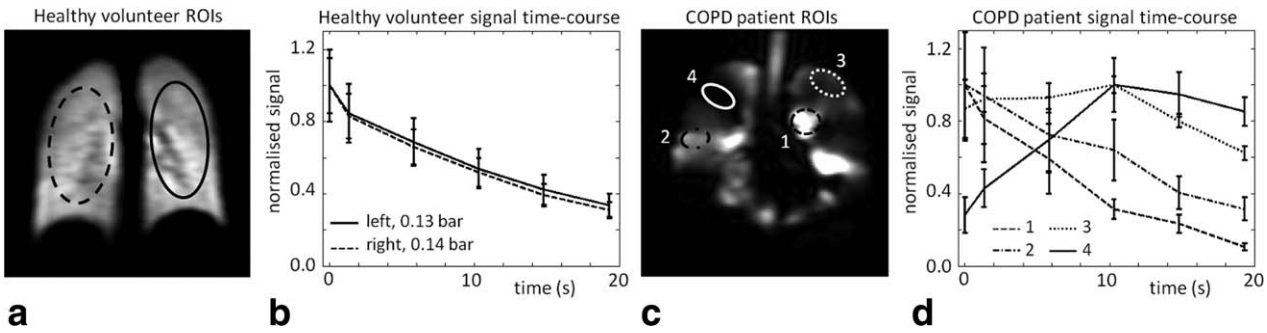

FIG. 4. Healthy volunteer (**a**) regions of interest and (**b**) normalized signal-time plots. COPD patient (**c**) regions of interest and (**d**) normalized signal-time plots; signal increases over time within the right ventilation defect (solid line) and left upper lobe (dotted line) ROIs. Mean pO_2 values for the COPD patient ROIs were (1) 0.17 bar, (2) 0.10 bar, (3) −0.10 bar, and (4) −0.40 bar. Error bars represent the standard deviation of the normalized signal.

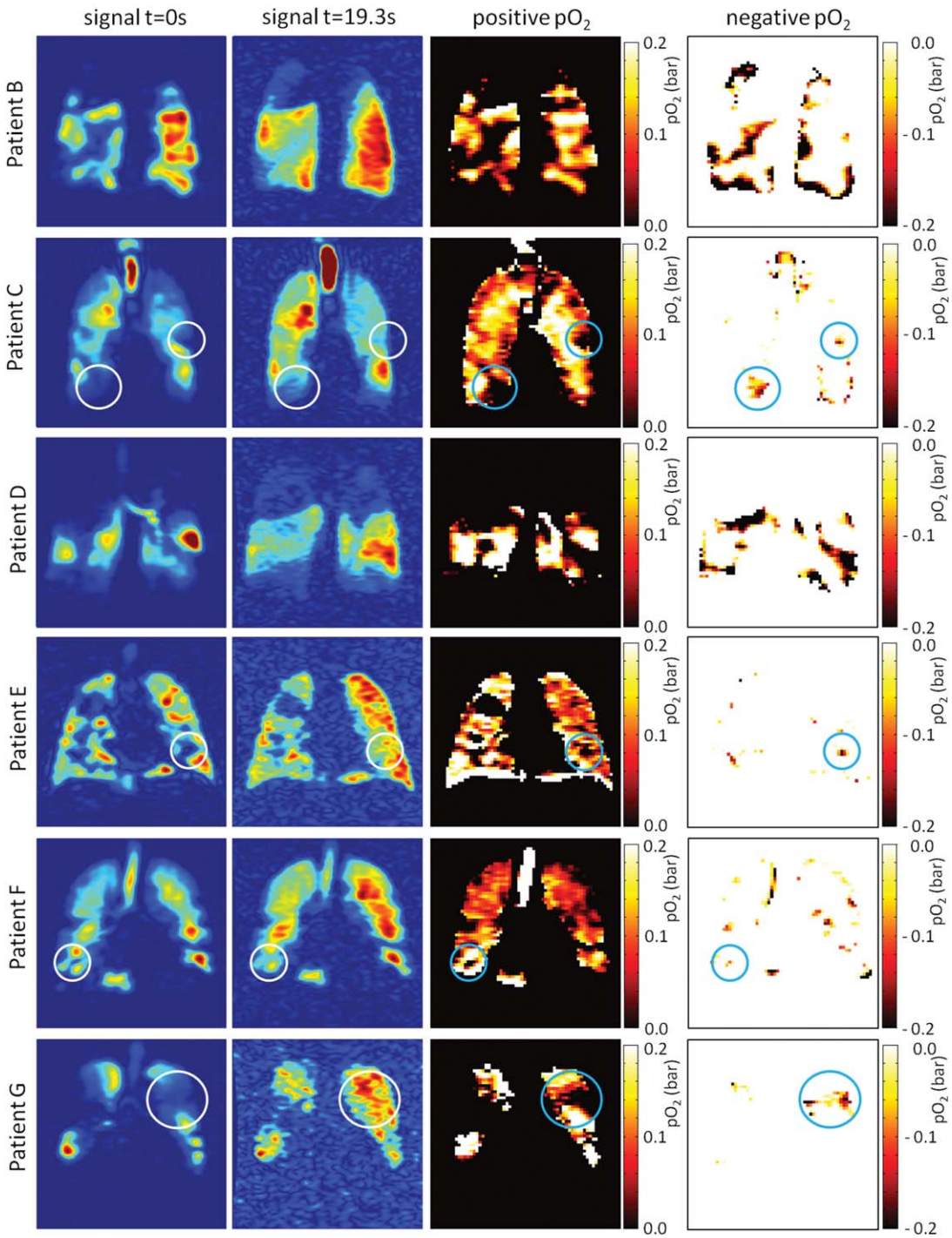

FIG. 5. Source images and calculated pO_2 maps from 9 COPD patients. Normalized signal at the first imaging time-point (column 1) and last imaging time-point (column 2). pO_2 maps showing positive (column 3) and negative (column 4) calculated pO_2 values. White circles highlight smaller regions where ^{3}He signal increased over time, resulting in negative pO_2 values (blue circles).

COPD patients. Defects, which were initially unventilated but filled with gas during the breath-hold, were seen in eight patients. Extensive ^{3}He movement during breath-hold was seen in four patients (A, B, D, and I) and regional increase in signal over time was seen to some extent in all patients, either in large areas (e.g., patient G) or small regions (e.g., patients F and J). A feature seen in several cases (e.g., patients D, F, and G) is two regions of high signal separated by a region of low signal which even out over time, causing high pO_2 values in the regions of originally high signal and negative pO_2 values in the region of originally low signal.

Some patients did not maintain a fully static breath-hold during the data acquisition, with their lung volume gradually decreasing over time, most likely due to involuntary relaxation of the diaphragm. Motion such as this also causes erroneous pO_2 values, which are most obvious where a region of ventilated tissue moves into

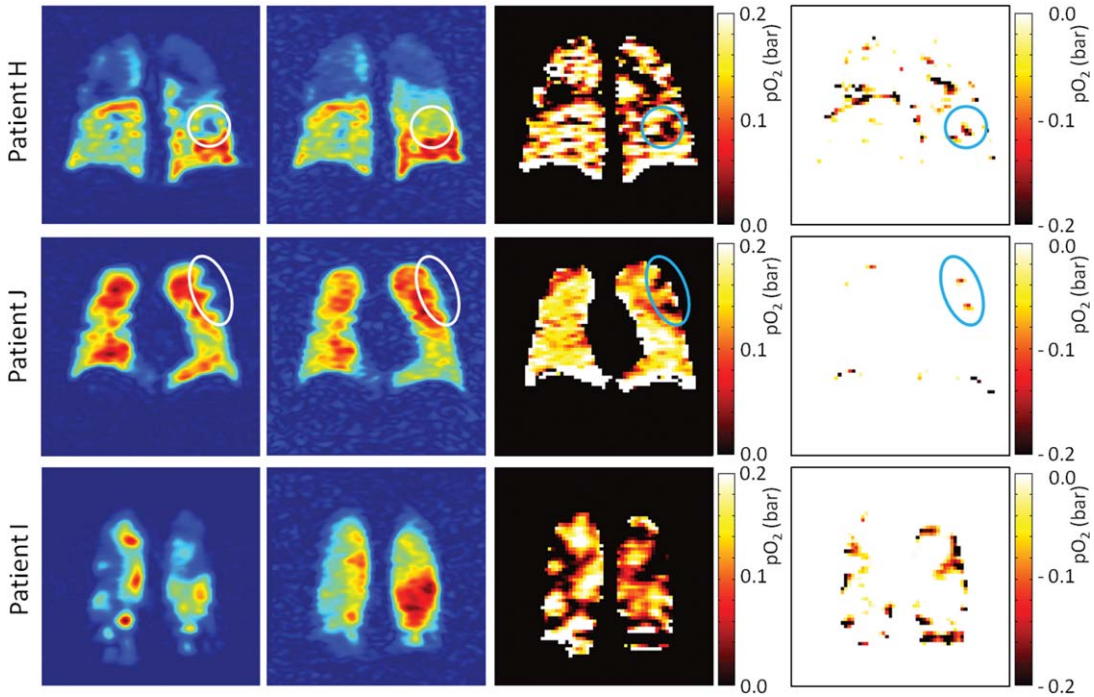

FIG. 5. (Continued)

an unventilated region causing negative pO_2 values or vice versa (i.e., near the diaphragm) which causes very high pO_2 values. This effect is demonstrated in patients H and I.

Mean negative pO_2 values of down to −0.30 bar were fitted from large regions of the images in patients A and D. The error in these negative pO_2 regions of lung in patients most affected by delayed-ventilation are substantially greater than the pO_2 values found in healthy lung. Not all patients were so strongly affected by delayed ventilation but all showed some regions of negative pO_2, which have an associated error of at least 100%. On the whole, the size of pO_2 measurement error was higher for regions of delayed ventilation with longer time to signal onset values. However, there were many voxels where the time to signal onset was zero but the signal still increased over time leading to negative pO_2 values.

The breath-hold time was found to have little effect on the measured pO_2 values in areas of negative pO_2. In regions of delayed ventilation, the signal increased over time at the beginning of the breath-hold, for example, the solid line in Figure 4d. In such a case, where signal increased for the first 10 s of breath-hold, a fit to the data would return a negative pO_2 value even if a short data acquisition were used such as in (13).

DISCUSSION

In this work, the linear oxygen-dependent signal decay model was used to estimate pO_2, which assumes signal decay to be dependent on oxygen-related T_1 relaxation and RF depolarization alone. Movement of gas within some regions of the lungs was found to alter the signal dynamics such that the signal behavior deviated significantly from that described by the linear model. More complex models of signal decay have been proposed recently which aim to estimate pO_2 more reliably, for example by adding a term to the linear oxygen-dependent model to account for gas redistribution (22). However, the separation of oxygen concentration and gas flow effects is not trivial, as they can both vary spatially and these spatio-temporal patterns are unknown and in many ways unique to the disruption of the lung microstructure in each patient's lungs. In addition, the two are intrinsically linked, as gas may travel between lung regions with different pO_2 values, which would affect the signal decay according to length of exposure to the different environments.

The negative pO_2 values estimated are a consequence of delayed-ventilation in these regions, causing signal to increase over time. Short-range ADC maps acquired from this group of patients showed that the degree of emphysema in regions of delayed-ventilation varied, and that severe emphysema sometimes but not always correlated with delayed ventilation. The regions of negative pO_2 were caused by the late inflow of gas rather than the elevated diffusion from the emphysematous nature of the tissue alone, although a particular instance of delayed-ventilation may be fundamentally linked to the presence of emphysema depending on the underlying mechanism of late ventilation.

The use of a 3D acquisition here mitigates pO_2 estimation errors caused by inter-slice diffusion mixing of gas with different polarizations, as addressed in (4). The errors in pO_2 estimation introduced by diffusion in this study are from diffusion of gas between voxels in highly emphysematous lung regions between time frames during data acquisition. When modeling diffusion in the

lungs, it is important to use the correct diffusion coefficient according to the time-length scale of the experiment and the underlying length scales of the physical structures within diseased lungs, which will depend on the severity and pattern of tissue destruction. On this time scale of seconds, ^{3}He diffuses over distances of millimeters within healthy lungs (as calculated with the representative long-range diffusion coefficient) and reflects the structure of the connections between alveoli. In severely emphysematous lungs of COPD patients, a wide range of long-range diffusion coefficients have been reported with an average of 0.24 cm^2/s (23), including many regions where $D > 0.4$ cm^2/s and some regions of bullous emphysema where D approached the free short time scale diffusion coefficient of ^{3}He in air (0.86 cm^2/s). The diffusion length in regions of unrestricted diffusion (large bullae where $D = 0.86$ cm^2/s) is 5.8 cm over the time period of 19.3 s used in this work, which is substantially greater than the voxel size of $0.55 \times 1.09 \times 2.0$ cm^3. This leads to diffusion of gas between voxels, and potentially between regions with different oxygen-concentrations, causing pO_2 mapping errors because the method assumes gas to be static during data acquisition.

It is difficult to assess the error of pO_2 estimates in patients with abnormal oxygen concentration distributions because the true pO_2 values are not known. The basic error analysis presented should not be overinterpreted. The magnitude of the physically unrealistic negative pO_2 values was used as a lower limit estimate of error in those regions, but perhaps more important are the unquantifiable errors in lung regions where signal still decreases over time but the influence of gas movement on that decay, and resulting pO_2 value, is unknown.

A study by Hamedani et al. proposing a multislice single breath-hold acquisition scheme to measure pO_2 (17) included discussion of the accuracy of ^{3}He pO_2 mapping in COPD. Regions of elevated and depressed pO_2 near each other and a non-negligible number of voxels with a derived pO_2 of zero were noted. These effects were observed particularly in the subject with COPD (of unstated disease severity) and also to a lesser extent in the current and former smokers. It was suggested that the technique could still be useful despite difficulty with strict interpretation of the resulting maps as pO_2. While the amount of error introduced depends on the amount of gas flow present, gas movement during breath-hold is a major limitation when mapping ^{3}He pO_2 in moderate to severe COPD, and may also prevent reliable pO_2 measurements in milder disease. However, observations of oxygen-weighted signal dynamics in a qualitative manner are useful to highlight regions of gas flow, and may provide valuable information even without absolute measurement of pO_2.

A case study of a patient with severe COPD (14) noted that the ^{3}He ADC was elevated and pO_2 was reduced in a ROI, from which it was suggested that oxygen exchange efficiency was reduced where lung tissue had been destroyed by COPD. However, a reduced pO_2 measurement would also be consistent with increased signal in later time points due to delayed-ventilation in the region of elevated ADC.

A short breath-hold ^{3}He pO_2 mapping technique such as that proposed by Miller et al. (13) would be less prone to errors due to gas movement because there is less time for gas redistribution to take place. However, there is still ^{3}He motion seen within the imaging delay time ($\Delta t = 2$–3 s) used for the short breath-hold technique in this patient group and a significant inter-image delay is needed for accurate quantification of T_1. Using the long range D values stated previously, with $\Delta t = 2.5$ s, gives an average $z_{rms} = 1.1$ cm (using $D = 0.24$ cm^2/s) increasing to a maximum $z_{rms} = 2.1$ cm where there is free diffusion (using $D = 0.86$ cm^2/s), which are lengths greater than or comparable with the in-plane voxel dimensions used in (13).

The gas movement seen during breath-hold in this group of COPD patients also has implications for ^{3}He static ventilation imaging. 2D multislice sequences are commonly used for high-resolution static ventilation imaging, with slices acquired consecutively during a breath-hold of ~10 s for full lung coverage. Where there is gas movement during breath-hold, slice-acquisition timing influences the resulting ventilation images. For example, if a slow-filling ventilation defect is imaged at the beginning of the breath-hold the region will appear unventilated, whereas if it is imaged at the end of the breath-hold it will appear ventilated. Image contrast depends on when the center of k-space is acquired for a 3D sequence also, but as the center of 3D k-space is only acquired once with a Cartesian trajectory all images will have $k = 0$ weighting from the same time point.

The lower diffusivity of ^{129}Xe may limit gas movement during breath-hold enough to make pO_2 measurements more reliable in COPD patients. ^{129}Xe in air is much less diffusive than ^{3}He in air with a free diffusion coefficient of 0.14 cm^2/s (7). This leads to a diffusion length scale on the order of pixel size for free diffusion, which would be much reduced for restricted diffusion. Experiments in guinea pigs found the T_1 of gas phase ^{129}Xe (31.3 ± 1.8 s) to be longer than that of ^{3}He (28.8 ± 1.8 s) in the lung (24), which would make slightly increased delay times more suitable to sample the T_1 decay of ^{129}Xe. However, the 6-fold reduction in diffusion coefficient would outweigh the effect of a small increase in delay time on root mean square displacement (z_{rms}). Conversely, the lower diffusivity of ^{129}Xe may introduce further delayed-ventilation in regions which would have become immediately ventilated with a ^{3}He/N_2 mix, and produce longer time constants in already established regions of delayed-ventilation. The solubility of xenon in parenchyma and blood would introduce another mechanism of signal loss unrelated to oxygen concentration. The percentage of dissolved to gaseous xenon is ~1–2% but it is in constant dynamic equilibrium with the gaseous xenon and the process is governed by subject-dependent physiological parameters (25).

CONCLUSIONS

It has been demonstrated in vivo that delayed-ventilation and/or diffusion limits the effectiveness of pO_2 mapping using the linear oxygen-dependent signal decay model in moderate to severe COPD, where movement of gas

within the lungs during breath-hold invalidates the assumption that all signal decay is due to T_1 decay and RF depolarization. We believe that lung pO_2 mapping with ^{3}He T_1 measurement is unreliable in patients with moderate to severe COPD in regions of lung showing delayed ventilation (19) or unrestricted diffusion (bullous emphysema), where inter-pixel gas movement within the lungs is significant on the time-scale of the experiment. Accurate separation and quantification of the effects of gas movement and oxygen concentration on the signal is highly challenging because the regional oxygen concentrations experienced by the gas are dependent on its pathway of movement through the lungs. Gas flow, gas diffusion, and oxygen concentration are all unknown and can be spatially varying and unique within different regions of diseased lung. Maps of signal change rate derived from time-resolved breath-hold images used for pO_2 mapping are useful to highlight regions of gas flow and are intrinsically affected by O_2 concentration.

REFERENCES

1. Deninger AJ, Eberle B, Ebert M, et al. Quantification of regional intrapulmonary oxygen partial pressure evolution during apnea by (3)He MRI. J Magn Reson 1999;141:207–216.
2. Deninger AJ, Eberle B, Ebert M, et al. (3)He-MRI-based measurements of intrapulmonary p(O_2) and its time course during apnea in healthy volunteers: first results, reproducibility, and technical limitations. NMR Biomed 2000;13:194–201.
3. Deninger AJ, Eberle B, Bermuth J, Escat B, Markstaller K, Schmiedeskamp J, Schreiber WG, Surkau R, Otten E, Kauczor HU. Assessment of a single-acquisition imaging sequence for oxygen-sensitive (3)He-MRI. Magn Reson Med 2002;47:105–114.
4. Wild JM, Fichele S, Woodhouse N, Paley MN, Kasuboski L, van Beek EJ. 3D volume-localized pO_2 measurement in the human lung with 3He MRI. Magn Reson Med 2005;53:1055–1064.
5. Saam B, Happer W, Middleton H. Nuclear relaxation of 3He in the presence of O_2. Phys Rev A 1995;52:862–865.
6. Cieslar K, Alsaid H, Stupar V, Gaillard S, Canet-Soulas E, Fissoune R, Cremillieux Y. Measurement of nonlinear pO_2 decay in mouse lungs using 3He-MRI. NMR Biomed 2007;20:383–391.
7. Chen XJ, Moller HE, Chawla MS, Cofer GP, Driehuys B, Hedlund LW, Johnson GA. Spatially resolved measurements of hyperpolarized gas properties in the lung in vivo. Part I: diffusion coefficient. Magn Reson Med 1999;42:721–728.
8. Owers-Bradley JR, Fichele S, Bennattayalah A, McGloin CJ, Bowtell RW, Morgan PS, Moody AR. MR tagging of human lungs using hyperpolarized 3He gas. J Magn Reson Imaging 2003;17:142–146.
9. Woods JC, Yablonskiy DA, Chino K, Tanoli TS, Cooper JD, Conradi MS. Magnetization tagging decay to measure long-range (3)He diffusion in healthy and emphysematous canine lungs. Magn Reson Med 2004;51:1002–1008.
10. Fichele S, Paley MN, Woodhouse N, Griffiths PD, van Beek EJ, Wild JM. Measurements and modeling of long range 3He diffusion in the lung using a "slice-washout" method. J Magn Reson 2005;174:28–33.
11. Wang C, Miller GW, Altes TA, de Lange EE, Cates GD Jr, Mugler JP III. Time dependence of 3He diffusion in the human lung: measurement in the long-time regime using stimulated echoes. Magn Reson Med 2006;56:296–309.
12. Gast KK, Biedermann A, Herweling A, Schreiber WG, Schmiedeskamp J, Mayer E, Heussel CP, Markstaller K, Kauczor HU, Eberle B. Oxygen-sensitive 3He-MRI in bronchiolitis obliterans after lung transplantation. Eur Radiol 2008;18:530–537.
13. Miller GW, Mugler JP III, Altes TA, Cai J, Mata JF, de Lange EE, Tobias WA, Cates GD, Brookeman JR. A short-breath-hold technique for lung pO_2 mapping with 3He MRI. Magn Reson Med 2010;63:127–136.
14. Yu J, Law M, Kadlecek S, Emami K, Ishii M, Stephen M, Woodburn JM, Vahdat V, Rizi RR. Simultaneous measurement of pulmonary partial pressure of oxygen and apparent diffusion coefficient by hyperpolarized 3He MRI. Magn Reson Med 2009;61:1015–1021.
15. Hamedani H, Emami K, Kadlecek SJ, et al. Reproducibility assessment of high resolution imaging of alveolar oxygen tension in human subjects. In Proceedings of the 19th Annual Meeting of ISMRM, Montreal, Canada, 2011. p. 930.
16. Xu Y, Hamedani H, Emami K, et al. Imaging regional heterogeneity of pulmonary oxygen tension as a diagnostic tool for obstructive lung diseases. In Proceedings of the 19th Annual Meeting of ISMRM, Montreal, Canada, 2011. p. 932.
17. Hamedani H, Kadlecek SJ, Emami K, et al. A multislice single breath-hold scheme for imaging alveolar oxygen tension in humans. Magn Reson Med 2012;67:1332–1345.
18. Swift AJ, Wild JM, Fichele S, Woodhouse N, Fleming S, Waterhouse J, Lawson RA, Paley MN, Van Beek EJ. Emphysematous changes and normal variation in smokers and COPD patients using diffusion 3He MRI. Eur J Radiol 2005;54:352–358.
19. Marshall H, Deppe MH, Parra-Robles J, Hillis S, Billings CG, Rajaram S, Swift A, Miller SR, Watson JH, Wolber J, Lipson DA, Lawson R, Wild JM, Direct visualisation of collateral ventilation in COPD with hyperpolarised gas MRI. Thorax 2012;67:613–617.
20. Wild JM, Teh K, Woodhouse N, Ireland R, Fichele S, Van Beek EJ, Paley MN. Single scan 3D pO_2 mapping with hyperpolarized 3He MRI. In Proceedings of the 14th Annual Meeting of ISMRM, Seattle, Washington, USA, 2006. p. 869.
21. Woodhouse N, Wild JM, Paley MN, Fichele S, Said Z, Swift AJ, van Beek EJ. Combined helium-3/proton magnetic resonance imaging measurement of ventilated lung volumes in smokers compared to never-smokers. J Magn Reson Imaging 2005;21:365–369.
22. Kadlecek S, Mongkolwisetwara P, Xin Y, Ishii M, Profka H, Emami K, Rizi R. Regional determination of oxygen uptake in rodent lungs using hyperpolarized gas and an analytical treatment of intrapulmonary gas redistribution. NMR Biomed 2011; 24:1253–1263.
23. Woods JC, Yablonskiy DA, Choong CK, Chino K, Pierce JA, Hogg JC, Bentley J, Cooper JD, Conradi MS, Macklem PT. Long-range diffusion of hyperpolarized 3He in explanted normal and emphysematous human lungs via magnetization tagging. J Appl Physiol 2005;99:1992–1997.
24. Moller HE, Chen XJ, Chawla MS, Driehuys B, Hedlund LW, Johnson GA. Signal dynamics in magnetic resonance imaging of the lung with hyperpolarized noble gases. J Magn Reson 1998;135:133–143.
25. Mugler JP III, Altes TA, Ruset IC, Dregely IM, Mata JF, Miller GW, Ketel S, Ketel J, Hersman FW, Ruppert K. Simultaneous magnetic resonance imaging of ventilation distribution and gas uptake in the human lung using hyperpolarized xenon-129. Proc Natl Acad Sci USA 2010;107:21707–21712.